InAsSb-based mid-infrared lasers (3.5-3.9 μm) and light-emitting diodes with AlAsSb claddings and semi-metal electron injection grown by metal-organic chemical vapor deposition

A. A. Allerman, R. M. Biefeld, and S. R. Kurtz

Sandia National Laboratory, Albuquerque, New Mexico, 87185, USA

ABSTRACT

Mid-infrared (3-5 μm) lasers and LED's are being developed for use in chemical sensor systems. As-rich, InAsSb heterostructures display unique electronic properties that are beneficial to the performance of these midwave infrared emitters. The metal-organic chemical vapor deposition (MOCVD) growth of $AlAs_{1-x}Sb_x$ cladding layers and InAsSb/InAsP superlattice active regions are described. A regrowth technique has been used to fabricate gain-guided, injection lasers using undoped (p-type) $AlAs_{0.16}Sb_{0.84}$ for optical confinement. In device studies, we demonstrate lasers and LEDs utilizing the semi-metal properties of a p-GaAsSb/n-InAs heterojunction as a source for injection of electrons into the active region of emitters. This avoids the difficulties associated with n-type doping of AlAsSb cladding layers required for conventional p-n junction lasers and also provides a means for construction of active regions with multiple gain stages. Gain guided injected lasers employing a strained InAsSb/InAs multi-quantum well active region operated up to 210 K in pulsed mode, with an emission wavelength of 3.8-3.9 μm. A characteristic temperature of 40 K was observed to 140 K and 29 K from 140 K to 210 K. An optically pumped laser with an InAsSb/InAsP superlattice active region is also described. The maximum operating temperature of this 3.7 μm laser was 240 K.

1. INTRODUCTION

Driven by chemical sensing and infrared countermeasure applications, several mid-infrared (2-6 μm) diode lasers with strained InAsSb active regions have been recently demonstrated. Devices with AlAsSb claddings have been grown by molecular-beam epitaxy,[1,2] and lasers with higher index, Al free InPSb claddings metal organic chemical vapor deposition (MOCVD) have also been reported.[3] Although AlAsSb claddings provide superior optical confinement, the large conduction band barriers associated with AlAsSb layers can result in poor electron injection and high turn-on voltages. Also, due to lack of satisfactory aluminum sources and residual carbon resulting in p-type doping of AlAsSb alloys, MOCVD growth of AlAsSb injection devices had not been reported. In this paper, we report MOCVD grown lasers with AlAsSb claddings. We describe an electrically injected device which utilizes a GaAsSb(p)/InAs(n) heterojunction to form an internal, semi-metal layer. The semi-metal acts as an internal electron source which can eliminate many of the problems associated with electron injection in these AlAsSb based devices. Furthermore, the use of an internal electron source enables us to consider alternative laser and LED designs that would not be feasible with conventional, p-n junction devices. Initial results for an optically pumped laser with an InAsSb/InAsP strained-layer superlattice (SLS) active region are also presented. Due to a large valence band offset, the light-heavy hole splitting in InAsSb/InAsP SLSs is estimated to be 80 meV, and Auger recombination should be further reduced in this active region.

DISCLAIMER

2. EXPERIMENT

This work was carried out in a previously described horizontal MOCVD system.[4] TMAA, or EDMAA, TESb, 100% and 10% arsine in hydrogen, and phosphine were the sources for Al, Sb, As and P respectively. $AlAs_{0.16}Sb_{0.84}$ layers 0.5 - 1 μm thick and lattice-matched to InAs were grown over a range of 500 to 600°C and 76 to 630 torr using a V/III ratio = 1.1 to 27 and an As/V ratio of 0.1 to 0.64 in the gas phase. The growth rate ranged between 0.35 - 2.0 $\mu m/hr$. The best morphology was achieved when grown on a buffer layer of InAs or an InAsSb/InAsP strained layer superlattice at a V/III ratio of 7.5 at 500 °C and 200 torr at 1.1 $\mu m/hr$.

Two active region structures were used for both laser diode and LED devices. The first consisted of a 10 period multi quantum well (MQW) structure of 90 Å InSbAs quantum wells with 450 Å InAs barriers. The other consisted of a 40 period strained layer superlattice (SLS) with the same InSbAs wells but with 85 Å InAsP barriers.

Secondary ion mass spectroscopy (SIMS) was used to determine C and O impurity concentrations. Five crystal x-ray diffraction (FCXRD) of the (004) reflection was used to determine alloy composition and superlattice period. Layer thickness was determined using a groove technique for thicker layers. Photoluminescence was used to characterize the optical quality of the active region structures.

3. GROWTH OF CLADDING AND ACTIVE REGION MATERIALS

The optimum growth conditions for $AlAs_xSb_{1-x}$ occurred at 500 °C and 200 torr at a growth rate of 1.1 $\mu m/hour$ using a V/III ratio of 7.5 assuming a vapor pressure of 0.75 torr for EDMAA at 19.8°C and an As/V flow ratio of 0.13. Surface morphology was strongly dependent on the InAs substrate. However, the use of a 30 period strain balanced InAsSb/InAsP SLS like that used for the active region greatly improved surface morphology. Surface roughness increased for growth rates of 2 $\mu m/hr$. for the same V/III and As/V conditions. Latticed matched GaAsSb cap layers were grown using similar conditions, a V/III of 6.2, and an As/V flow ratio of 0.071. Five crystal x-ray diffraction (FCXRD) measurements of lattice matched AlAsSb films typically exhibited full widths at half of the maximum intensity (FWHM) less than 100 arc seconds. We were also able to reproducibly obtain lattice matching of $AlAs_xSb_{1-x}$ to InAs to within less than 0.015 percent using EDMAA.

The use of other than the above stated growth conditions led to problems in compositional control and reproducibility during the growth of $AlAs_xSb_{1-x}$ layers lattice matched to InAs. Growth at 600 °C resulted in a very broad x-ray peak that extended over hundreds of arc seconds with a constant intensity. Analysis of the x-ray spectra indicated that the large peak width was due to a variation of Sb composition that occurred in the layer as it was grown. Broad x-ray peaks were also observed in films grown using TMAA. The transport of TMAA from the solid source varied during the growth run and changed the V/III ratio resulting in x-ray peaks several hundred arc seconds wide. Sb was also detected by x-ray diffraction in InAs layers grown at 600 °C following previous growths of AlAsSb. We suspect that evaporation of elemental Sb, which has a vapor pressure of 0.1 torr at 600 °C, from deposits on the chamber wall results in the compositional drift observed in the AlAsSb layers grown at 600 °C. Growth at 500 °C greatly reduces this effect as x-ray peaks with FHWM of less than 100 arc seconds were routinely achieved. Likewise Sb was not detected by x-ray diffraction in InAs layers grown following AlAsSb growths. Growth at 70 or 500 torr yielded broader x-ray diffraction peaks (FWHM 300 arc seconds) with less reproducible lattice matching.

SIMS analysis of undoped AlAsSb showed the oxygen level to be 1.2×10^{19} cm^{-3} for a film grown at 500 °C and 200 torr using EDMAA. A similar level of oxygen (1.6×10^{19} cm^{-3}) was found in a film grown at 600 °C and 200 torr using TMAA. The level of carbon found in the film grown at 600 °C was 7.3×10^{17} cm^{-3} and was much lower than the 2.6×10^{18} cm^{-3} found in the sample grown at 500 °C. The source of the oxygen found in these materials is unknown at this time. The oxygen could be coming from contaminants in the organometallic sources, the background O in the MOCVD reactor, or from reaction of the samples with air.

The details of the growth of the InAsSb/InAs multiple quantum well (MQW) structures on InAs have been previously published.[5] An x-ray diffraction pattern of an InAs/InAs$_{0.89}$Sb$_{0.11}$ MQW grown on InAs had sharp satellite peaks out to n=7 indicating good crystalline structure. The structure was grown at 500 °C, 200 torr, a V/III ratio of 25 with an As/V ratio of 0.75 and a growth rate of 2.5 Å/second. A 15 second purge time with reactants switched out of the chamber was used between each layer. The composition, X, of the InAs$_{1-x}$Sb$_x$ quantum wells could be varied between X = 0.1 and 0.2 by changing the As/V ratio between 0.81 and 0.63 using these growth conditions. The composition changes can be explained by the use of a thermodynamic model as previously discussed.[5]

InAsP layers were grown using 10% AsH$_3$ in hydrogen with a V/III ratio of 216 and a As/V ratio of .016. The high V/III and low As/V ratios reflect the low thermal decomposition efficiency of PH$_3$ at 500 °C and 200 torr. The growth rate was 2.5 Å/sec. in the active region.

Low temperature (< 20 K) photoluminescence emission could be controlled between 3.9 to 6.0 μm for Sb compositions between 0.11 to 0.20 in the InAsSb/InAs MQW structures grown on InAs. The long wavelength deviation of these bandgap values from those previously published may be explained by the CuPt-type ordering and phase separation found in these materials.[6, 7] Previous work has shown that the InAs/InAsSb interface band offset in these MOCVD grown materials is type I.[8] PL emission from InAsSb/InAsP SLS structures were blue shifted due to the added confinement provided by the InAsP barriers (Figure 1). PL emission was observed between 3.1 to 4.2 μm for the 20 period SLS shown in Figure 1.
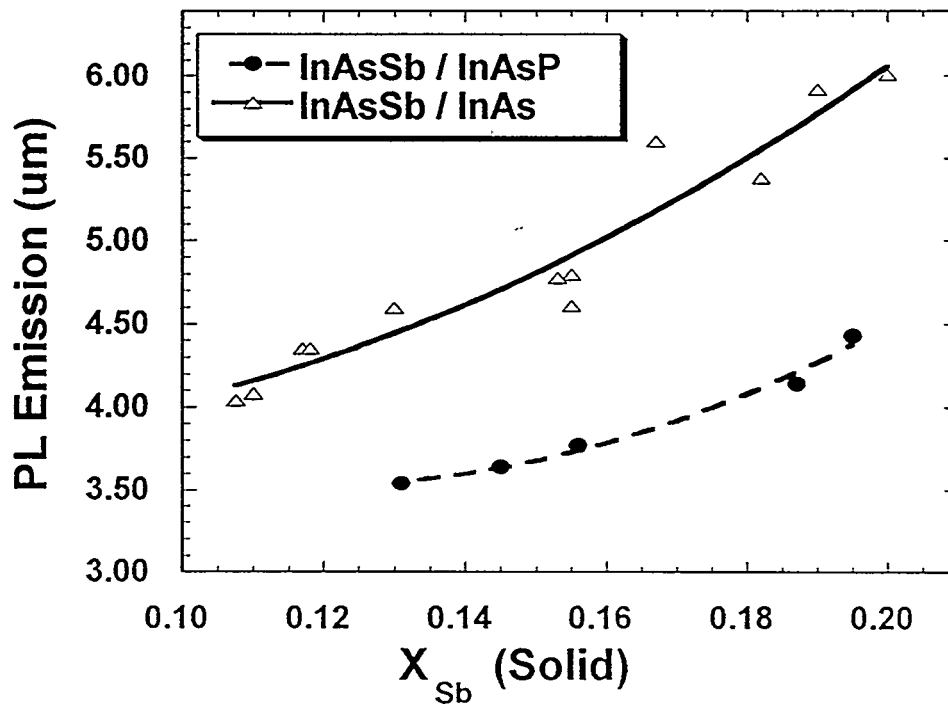

Figure 1. Low temperature photoluminescence (< 20K) from 10 period 90Å InSb$_x$As$_{1-x}$ / 450Å InAs MQW's and 40 period 75Å InSb$_x$As$_{1-x}$ / 84Å InAs$_{.76}$P$_{.24}$ SLS's grown on InAs.

FCXRD of a 20 period InAsSb/InAsP SLS shows sharp SL peaks indicating good structural quality. The n=0 peak is within 10 arc seconds of the substrate indicating the structure is strain balanced. PL emission for the structure grown on InAs is observed at 3.61 µm at 16 K and red shifts to 4.15 µm at 300 K with 8% of the peak intensity at 16 K.

Although the independent growth of the $AlAs_xSb_{1-x}$ layers or the MQW structures gave uniform and reproducible x-ray diffraction patterns, only a very broad x-ray diffraction pattern was observed when the MQW was grown sequentially on top of the $AlAs_xSb_{1-x}$. When a layer of InAs was grown after a layer of lattice matched $AlAs_xSb_{1-x}$, a broad x-ray peak was observed at two theta values greater than the InAs substrate. SIMS measurements indicated the presence of Al in the InAs layer. In order to avoid the incorporation of Al into the quantum well structures, we developed a regrowth technique. Following the growth of the 2.5 µm $AlAs_xSb_{1-x}$ confinement layer capped with 500 Å of $GaAs_{1-x}Sb_x$ and a 400 Å layer of InAsSb, the quartz reaction chamber was cleaned before growing the rest of the laser structure. The second growth starts with the active region followed by a second 2.5 µm confinement layer of $AlAs_xSb_{1-x}$ followed by a 1200 Å contact layer of GaAsSb.

None of the layers in the laser structure were intentional doped. The semi-metal nature of the p-GaAsSb / n-InAs interface grown at the end of the first growth is used to inject electrons into the active region. The satellite peaks observed in the first growth are from the InAsSb/InAsP SLS used as a buffer to improve surface morphology. The same structure used in the active region was also used for the buffer. The cladding layer is closely lattice-matched to the substrate.

4. SEMI-METAL INJECTION LASER WITH PSEUDOMORPHIC InAsSb MULTIPLE QUANTUM WELL ACTIVE REGION

The band alignments [9] for the injection laser are shown in Figure 2. As confirmed by x-ray measurements, both the claddings and active region of the laser are nominally lattice matched to the substrate. Following a $GaAs_{0.09}Sb_{0.91}$ buffer, a 2.5 µm thick $AlAs_{0.16}Sb_{0.84}$ cladding is grown on an n-type, InAs substrate. A 200 Å, $GaAs_{0.09}Sb_{0.91}$ layer lies between the bottom cladding and a 0.6 µm thick InAs active region containing 10, pseudomorphic $InAs_{0.88}Sb_{0.12}$ quantum wells, each 90 Å thick. A 2.5 µm thick $AlAs_{0.16}Sb_{0.84}$ cladding followed by a 1200 Å, $GaAs_{0.09}Sb_{0.91}$ contact and oxidation barrier layer is grown on top of the active region. AlAsSb and GaAsSb alloys have p-type background doping levels of 10^{17} /cm^3, estimated from Hall measurements. The background doping of the InAs/InAsSb active region is n-type, 10^{15}-10^{16} /cm^3. Details of the MOCVD growth are published elsewhere.[5,10]
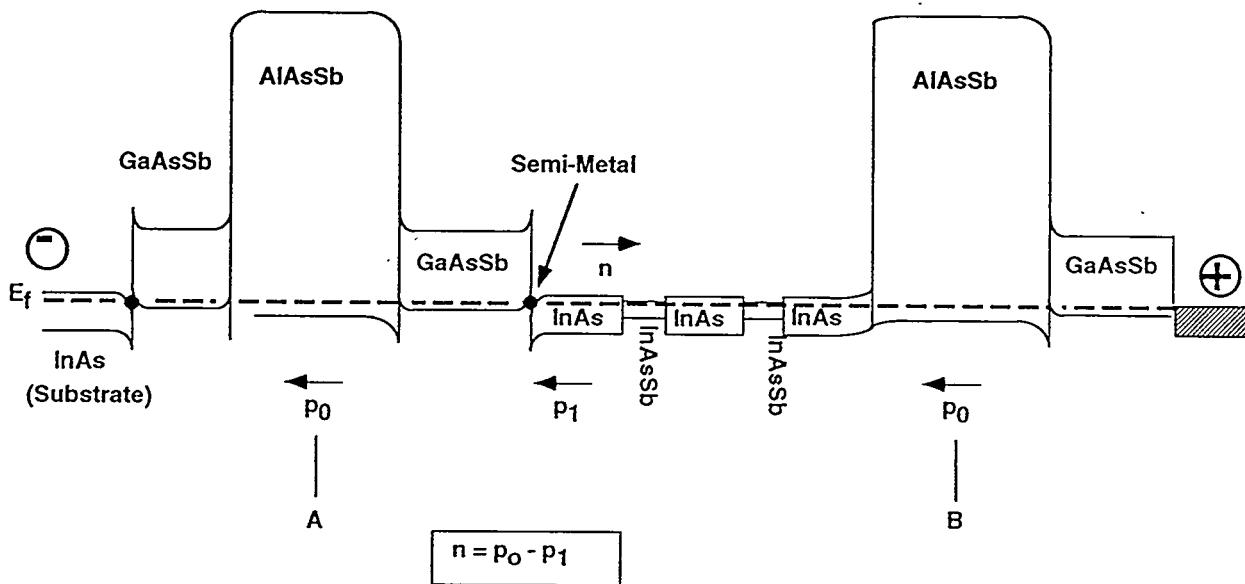

Figure 2. Heterojunction band alignments for the MOCVD-grown, injection laser with a pseudomorphic InAsSb MQW active region. Forward bias polarity is indicated in the figure.

For a wide range of Fermi energies, the GaAsSb (p) / InAs (n) heterojunction is a semi-metal, acting as a source/sink for electron-hole pairs. In forward bias (Figure 2), electrons are generated in the semi-metal and swept into the active region to recombine with holes being injected from the anode (+). The hole flux is replenished by holes generated in the semi-metal and swept away from the active region. Only hole transport is observed in the AlAsSb claddings (labeled points A and B in Figure 2), and over this segment, the device can be described as unipolar.

Gain-guided, stripe lasers were fabricated with Ti (50 Å) / Au (4000 Å) metallizations. The facets were uncoated. Under pulsed operation, lasing was observed in forward bias with 40x1000 or 80x1000 micron stripes. No emission occurred under reverse bias. Devices were tested with 100 nsec pulse widths at 10 kHz (0.1 % duty-cycle). Several longitudinal modes were observed in the 3.8-3.9 μm range for 80 K and 200 K operation. Characteristic of the pseudomorphic InAsSb lasers, laser emission was blue-shifted by 20 meV from the peak of the InAsSb quantum well photoluminescence, [3] and consistent with the selection rule for the compressively strained InAsSb quantum well electron ($|1/2,\pm1/2>$) -hole ($|3/2,\pm3/2>$) transition, laser emission was 100% TE polarized. The lasers displayed sharp threshold current characteristics, and lasing was observed through 210 K. (Figure 3) Under pulsed operation, peak power levels 1 mW/facet could be obtained. A characteristic temperature (T_o) in the 30-40 K range was observed, with the lower value (30 K) being misleading due to degradation of the device.
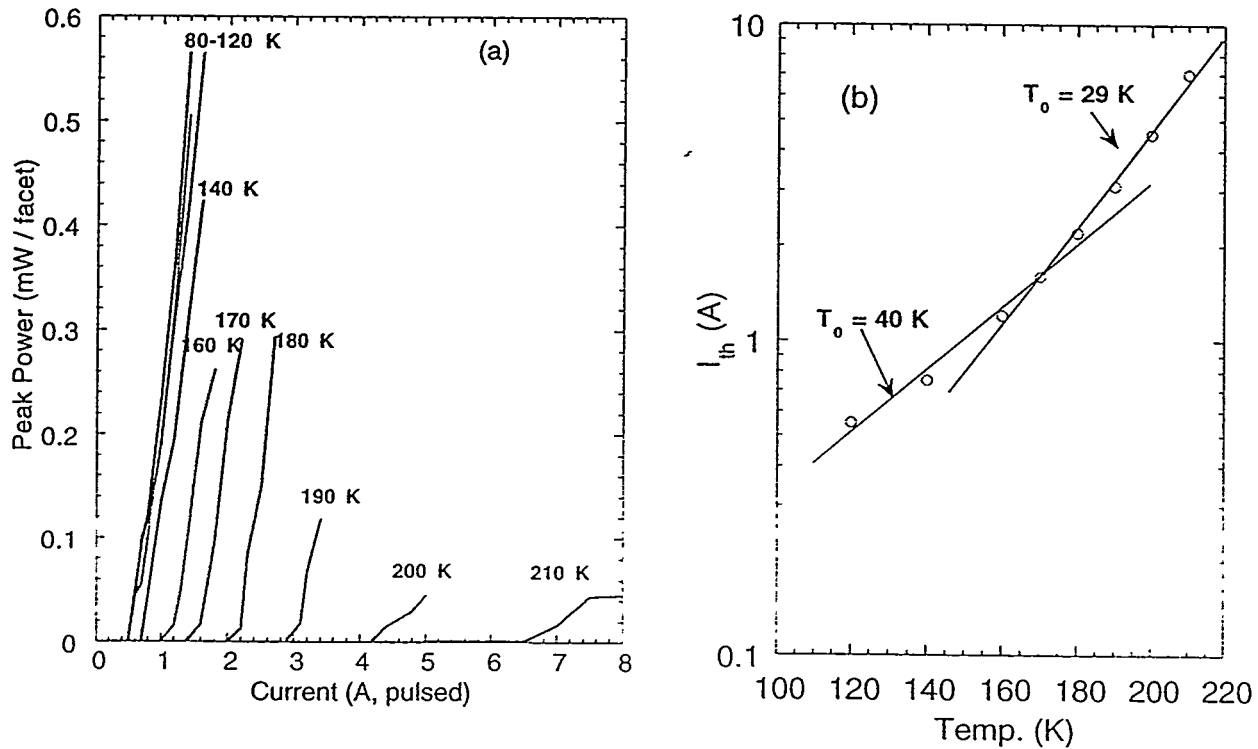

Figure 3. (a) Injection laser emission intensity versus peak current for various temperatures. (b) Pulsed threshold current versus temperature. The stripe dimensions were 40x1000 μm.

These maximum operating and characteristic temperature values are comparable to the highest values reported to date, for injection lasers of this wavelength with either strained InAsSb or InAs/GaInSb active regions.[2,3,11] Previously, a bipolar laser with a similar, pseudomorphic InAsSb multiple quantum well active region displayed the same characteristic temperature.[3] We believe that the characteristic temperature of both devices is limited by design of the active region and the resulting Auger rates.[3] Unlike bipolar lasers, cw operation of the unipolar laser has not yet been observed. At threshold and 100K, we find that the maximum duration of the unipolar laser output is 10^5 sec, with a comparable recovery time. If the device is driven above threshold with long pulses, lasing ceases and a different, low intensity emission spectrum is observed which indicates extreme band bending and depletion of the semi-metal. Due to capacitive charging within the device, the threshold current of the semi-metal laser was 10x that reported previously for the pseudomorphic, bipolar laser. Lasing pulse duration, duty-cycle, threshold current, and turn-on voltage of the semi-metal emitters may be improved with modifications in doping and heterojunction design.

5. OPTICALLY PUMPED, InAsSb/InAsP SLS ACTIVE REGION LASER

To further reduce Auger recombination, we are developing lasers with InAsSb/InAsP SLS active regions. Based on band offsets and light-heavy hole splittings measured in other InAsSb heterostructures,[8,12] we find that InAsSb/InAsP SLSs will exhibit large electron and hole confinement energies, and light-heavy hole splittings as large as 80 meV should be easily realized. (Figure 4) We constructed a InAsSb/InAsP SLS laser similar to the semi-metal injection laser described previously, except a $InAs_{0.88}Sb_{0.12}/InAs_{0.73}P_{0.27}$ (80 Å / 80Å) SLS was substituted in place of the pseudomorphic active region. The unnecessary carriers in the cladding layers and the semi-metal layer may contribute loss to this optically pumped device.
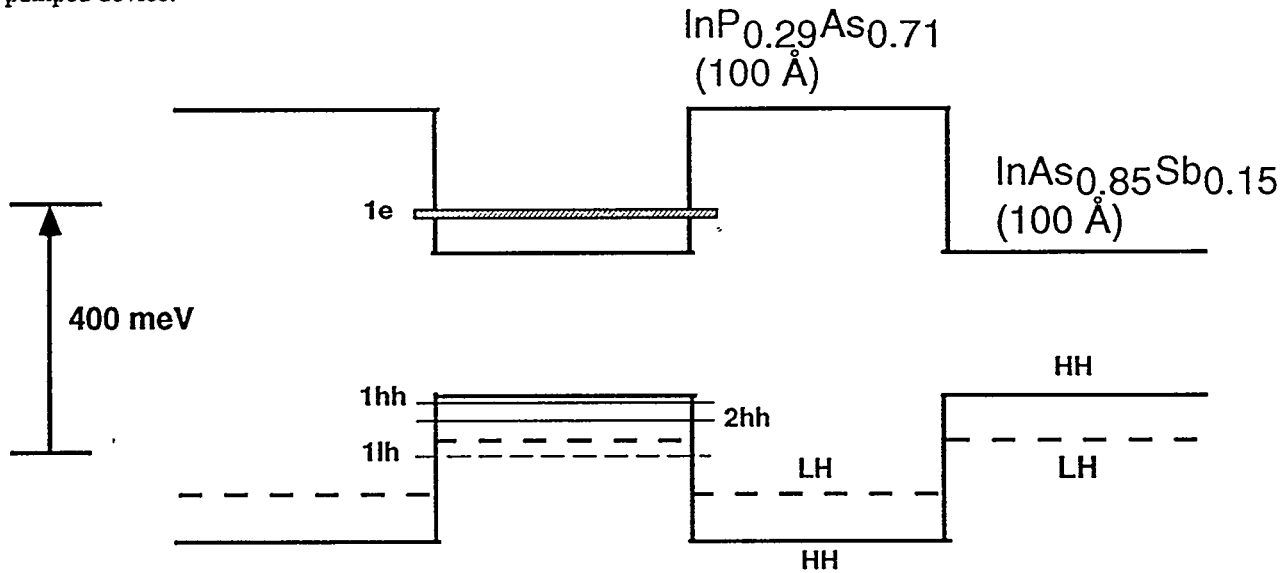
$$E (1e - 1hh) = 303 \text{ meV} (4.1 \text{ μm})$$

$$E (1hh - 1lh) = 86 \text{ meV}$$

SLS lattice- matched to InAs

Figure 4 - Band alignments and quantum confinement state energies (drawn to scale) for an $InAs_{0.85}Sb_{0.15}$ / $InAs_{0.71}P_{0.29}$ (100 Å / 100 Å) SLS. The estimated bandgap of the unstrained, MOCVD-grown $InAs_{0.85}Sb_{0.15}$ alloy was 218 meV.

The InAsSb/InAsP SLS laser was pumped with a Q-switched Nd:YAG (20 Hz, 10 nsec pulse), and emission was detected with an FTIR operated in a step-scan mode. Due to the low rep-rate of the pump, the resolution of the experiment was 2 cm^{-1}. Laser emission was observed from cleaved bars, 1000 μm wide. A sharp lasing threshold and spectrally narrowed stimulated emission was seen from 80 K through 240 K, the maximum temperature where lasing occurred. The temperature dependence of the threshold is well described by a characteristic temperature, $T_0 = 32$ K. Unlike the pseudomorphic devices, laser emission occurs near the peak of the spontaneous emission, indicated by the photoluminescence spectrum in Figure 5. The wavelength of the SLS laser shifts from 3.5 μm to 3.7 μm due to the decrease in bandgap over the 80-240 K temperature range. Overall, the performance (output power, threshold power, characteristic temperature, maximum temperature) of the optically pumped type I, InAsSb/InAsP SLS laser is comparable to that initially reported for a 4 μm, InAs/GaInSb type II laser measured under similar conditions.[13]
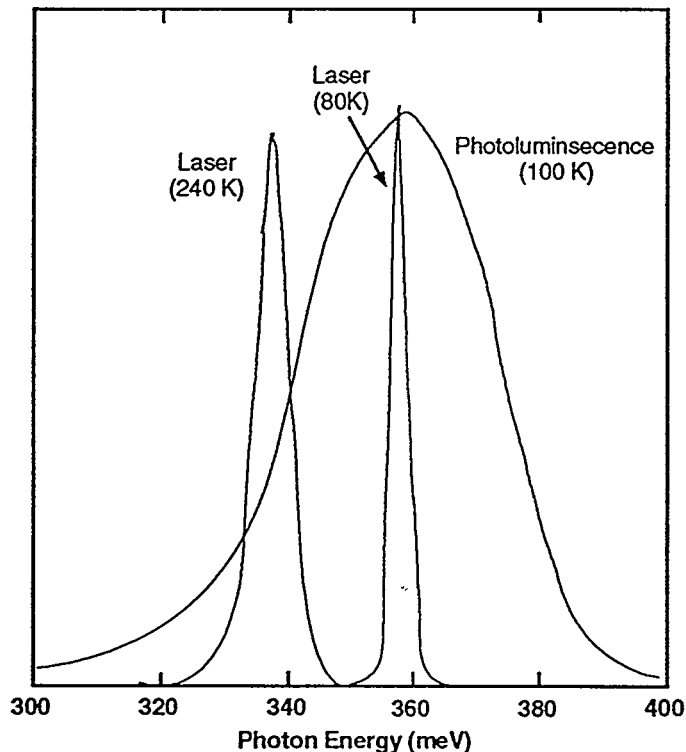

Figure 5 - Photoluminescence and optically pumped laser emission spectra for a device with an $InAs_{0.88}Sb_{0.12}/InAs_{0.73}P_{0.27}$ (80 Å / 80 Å) SLS active region.

6. CONCLUSIONS

We have grown $AlAs_xSb_{1-x}$ epitaxial layers by metal-organic chemical vapor deposition (MOCVD) using trimethylamine alane or ethyldimethylamine alane, triethylantimony, and arsine. The growth of high quality $AlAs_xSb_{1-x}$ by MOCVD has been demonstrated and used for optical confinement layers in a 3.8-3.9 μm injection laser with a novel GaSb/InAs semi-metal electron injector. The use of the InAs/GaSb semi-metal for carrier injection, and the compatibility of the semi-metal with InAsSb devices is unique. Diode lasers employing InAsSb/InAs MQW active regions have operated under electrical injection (pulsed) to 210 K. Optically pumped laser structures employing strain balanced InAsSb/InAsP SLS active regions have operated to 240 K under pulsed conditions.

7. ACKNOWLEDGEMENTS

8. REFERENCES

[1] H. K. Choi and G. W. Turner, Appl. Phys. Lett. 67, 332 (1995).

[2] Y-H. Zhang, Appl. Phys. Lett. 66, 118 (1995).

[3] S. R. Kurtz, R. M. Biefeld, A. A. Allerman, A. J. Howard, M. H. Crawford, and M. W. Pelczynski, Appl. Phys. Lett. 68, 1332 (1996).

[4] R.M.Biefeld, C.R. Hills, and S.R. Lee, J. Crys. Growth 91, 515 (1988).

[5] R. M. Biefeld, K. C. Baucom, and S. R. Kurtz, J. Crystal Growth, 137, 231 (1994).

[6] D. M. Follstaedt, R. M. Biefeld, S. R. Kurtz, and K. C. Baucom, J. Electronic Mater. 24, 819 (1995).

[7] S. R. Kurtz, L. R. Dawson, R. M. Biefeld, D. M. Follstaedt, and B. L. Doyle, Phys. Rev. B, 46, 1909 (1992).

[8] S. R. Kurtz, R. M. Biefeld, and A. J. Howard, Appl. Phys. Lett., 67, 3331 (1995).

[9] Chris G. Van de Walle, Phys. Rev. B 39, 1871 (1989).

[10] A. A. Allerman, R. M. Biefeld, and S. R. Kurtz, Appl. Phys. Lett. 69, 465 (1996).

[11] R. H. Miles (private communication).

[12] S. R. Kurtz and R. M. Biefeld, Appl. Phys. Lett. 66, 364 (1995).

[13] J. I. Malin, J. R. Meyer, C. L. Felix, J. R. Lindle, L. Goldberg, C. A. Hoffman, F. J. Bartoli, C. H. Lin, P. C. Chang, S. J. Murry, R. Q. Yang, and S. S. Pei, Appl Phys. Lett. 68, 2976 (1996).